Unusual percolation in simple small-world networks

Reuven Cohen,[1] Daryush Jonathan Dawid,[2] Mehran Kardar,[3] and Yaneer Bar-Yam[4]
[1]*Department of Mathematics, Bar-Ilan University, Ramat-Gan 52900, Israel*
[2]*Brick Court Chambers, Essex Street, London WC2R 3LD, United Kingdom*
[3]*Department of Physics, Massachusetts Institute of Technology, Cambridge, Massachusetts 02139, USA*
[4]*New England Complex Systems Institute, Cambridge, Massachusetts 02138, USA*
(Received 7 February 2008; revised manuscript received 4 May 2009; published 23 June 2009)

We present an exact solution of percolation in a generalized class of Watts-Strogatz graphs defined on a one-dimensional underlying lattice. We find a nonclassical critical point in the limit of the number of long-range bonds in the system going to zero, with a discontinuity in the percolation probability and a divergence in the mean finite-cluster size. We show that the critical behavior falls into one of three regimes depending on the proportion of occupied long-range to unoccupied nearest-neighbor bonds, with each regime being characterized by different critical exponents. The three regimes can be united by a single scaling function around the critical point. These results can be used to identify the number of long-range links necessary to secure connectivity in a communication or transportation chain. As an example, we can resolve the communication problem in a game of "telephone."

DOI: 10.1103/PhysRevE.79.066112 PACS number(s): 89.75.Hc, 05.50.+q, 02.50.−r, 64.60.De

I. INTRODUCTION

A. Small-world networks

In a 1967 study on social networks [1], Stanley Milgram found that on average a randomly chosen person in the midwest USA could be connected to a target person in Massachusetts through a string of first-name acquaintances in only six steps. While this notion of "six degrees of separation" rapidly acquired folkloric status in popular culture [2], the structure of the underlying networks remained largely unexplored until recently. The "smallness" was attributed to the logarithmic scaling with graph size of distances between nodes on random graphs [3]. Actual social networks are far from random, however. Today, social and other networks are frequently described as consisting of mutually interconnected local groups together with some far-flung ties [4]. Interest in the properties of such partially ordered networks was sparked by the work of Watts and Strogatz [5], who in 1998 introduced and studied numerically a "small-world" network model in which a controlled degree of disorder is introduced into initially ordered graphs by randomly rewiring some fraction of their links. A schematic representation of a small-world graph is depicted in Fig. 1(b).

Watts and Strogatz's observation that even a small degree of randomness changes the scaling of the minimum graph distance between randomly chosen nodes, l, with the total number of nodes, N, from the linear behavior of ordered graphs to the logarithmic scaling associated with random graphs provoked a flurry of interest. The scale dependence of l has been obtained by renormalization-group [6] and mean-field analysis [7]. In particular, Moukarzel [8] showed that for systems of size L on a d-dimensional underlying lattice there is a crossover length $r_c \sim \log(pL)$, where p is the density of shortcuts, such that, on a scale $r < r_c$, $l(r)$ scales as r, whereas on larger scales $l(r) \sim r_c$.

Today, the term small world has come to describe any system displaying a combination of strong local clustering with a small graph diameter. Mathias and Gopal [9] have shown that optimization of a regular graph for high connectivity and low total bond length gives rise to small-world behavior. Interestingly, the optimized graphs are distinguished by the generation of a relatively small number of highly connected "hub" vertices rather than a random distribution of long-range links as in the Watts-Strogatz (WS) model. Hub-dominated networks are also generated by a model for a dynamically expanding graph proposed by Barabási and Albert [10] to explain the scale-free (i.e., power-law) distribution in vertex connectivity common to

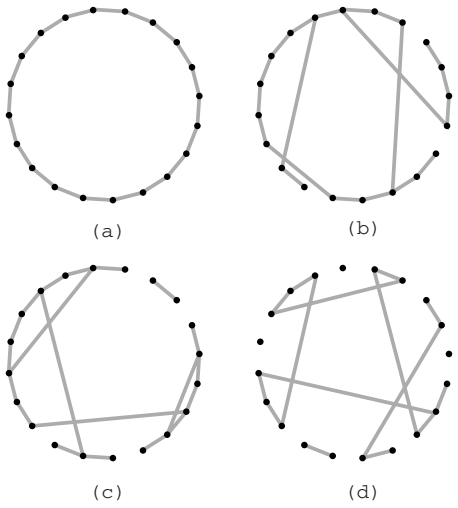

FIG. 1. Examples of small-world graphs: (a) a fully connected ordered ring with $N=20$ vertices. (b) A graph generated by the original Watts-Strogatz algorithm with $k=1$ and $p_l=\phi=1/5$, giving $p_s=4/5$. Note that every long-range link is created by reattaching the far end of the broken short-range link. (c) The Watts-Strogatz variant used for analytical calculations. Again $k=1$ and $\phi=1/5$ but this time the addition of long-range bonds and deletion of short-range bonds is carried out independently; this makes the appearance of disconnected (finite) clusters more likely but does not prevent the appearance of small-world behavior. (d) A generalized Watts-Strogatz graph with $k=1$, $p=p_l=1/4$, and $n=1/2$, giving $p_s=1/2$.

many real-world networks, such as the world-wide web and the science citation database. For scale-free networks, it has been shown [11–13] that the network is even smaller than small-world networks, i.e., has a sublogarithmic average distance between nodes. A further study of real-world networks by Amaral *et al.* [14] discerned two other classes of behavior in small-world networks in addition to scale-free graphs, characterized by truncated power-law and rapidly decaying connectivities, respectively, and proposed how such behavior can arise due to constraints placed on the Albert-Barabási model.

In addition to work on the properties of small-world networks themselves, recent attention has focused on the behavior of physical systems defined on small-world graphs, including Ising models [15,16], neural networks [17], and random walks [18,19]. There has also been work on models of disease epidemics using site and bond percolation defined on small-world graphs (see, e.g., Refs. [20–22]) as described below. Evolving contagion processes on small-world networks have been investigated in Ref. [23], and the dynamical response of complex networks due to external perturbations is studied in Refs. [24,25]. The analysis of implications of small-world networks for goal directed social network behavior is presented in Ref. [26]. Results for searching in small-world networks can be found in [27,28]. For some contemporary reviews of small-world networks and networks in general, see, e.g., Refs. [29–33].

The wide ranging interest and implications of small-world networks have also led to a need for precise understanding and, where possible, exact solutions of the fundamental properties of these networks. In this paper we focus on identifying unusual properties that arise in the case of small-world networks on an underlying one-dimensional lattice. We provide exact solutions for a generalized model and study the behavior in the limit of few long-range links—a limit we find is very sensitive to the manner in which it is obtained. We also point to practical implications for securing connectivity in one-dimensional transportation and communication chains, showing how failure of some local links is overcome by the existence of long-range links.

B. Percolation on small-world graphs

Percolation is quite sensitive to the geometry of the underlying lattice. One-dimensional lattices are generally inappropriate for representing the graph underlying social networks; however, they may be appropriate in specific contexts. Consider, for instance, a chain of islands, cities, or nodes in an *ad hoc* or wired network situated in a nearly linear formation, say along a road. Such a configuration is extremely sensitive to breakdown, if even a small number of the links connecting the nodes is removed. This follows from the well-known result that one-dimensional systems only percolate in the limit of zero failure rate. To fortify the structure of such a network, random long-range links may be added that can backup missing short-range bonds. For road transportation long-range bonds may be added by airlines or boat lines while for wired communications long-range bonds might be provided by microwave or satellite communication links. The important question: "how many long-range links are needed to replace an (expected) number of short-range failed links?" is addressed in this paper. It should be noted that a similar problem for square lattices was studied in Ref. [34].

For a simple ring structure it will be shown that, for any constant ratio of long-range bonds added to replace removed short-range bonds, some nodes remain isolated from the rest. However, if only a quarter of the number of the failed short-range bonds exist as long-range shortcuts, the chain is not broken—a giant connected component exists comprising a constant fraction of the nodes.

As an example, this shows how to achieve reliable communication in a game of "telephone." In the game, one person tells a second person something, the second tells a third, and so on down a chain. For a long chain, and even a reasonably short chain, errors garble the communication. Our results show that if there are also long-range links of communication along the chain, comprising a quarter of the short-range links, the random errors that are formed do not cause errors in the answer.

We note the difference in behavior of short-range and long-range fortifying links. Short-range fortification in a k-ring architecture, in which each node is connected to its $2k$ nearest neighbors leads to an exponentially decreasing probability of disconnection in k. Still, in the limit of long enough chains, a fixed k implies that a chain always breaks. Moreover, this method of reinforcement is expensive in the number of links needed. The probability of a node being disconnected from all nodes in one direction is p^k. This is a lower bound on the probability of a break in the chain at some node. This probability is independent for nodes that are k hops apart. The probability of a chain starting at some node to be at least of length n is bounded by $(1-p^k)^{n/k}$. This decays exponentially with n. Therefore, for constant p and k, the probability of finding a chain of length of order N is vanishingly small unless $k=O(\ln N)$. Thus, resiliency to random failure requires at least $O(N \ln N)$ bonds (corresponding to the known collapse of the one-dimensional percolation), whereas, as will be seen, the number of long-range links needed is linear in N (and actually lower than N). It should be noted that, however, for random long-range bonds, $O(N \ln N)$ bonds are still needed to ensure that all nodes are connected [3].

The best practical solution may be to combine short-range and long-range reinforcements. We find that, for $k>1$, and small removal rates of the short-range bonds, the network will remain connected (up to a statistically insignificant fraction of the nodes) for any constant ratio of added long-range bonds. Thus, the addition of relatively few random long-range bonds can ensure percolation and global connectivity.

Recent studies of percolation on small-world networks [35] have antecedents in the study of bond percolation [36] whose methodology is the basis of our analysis. Small-world-type graphs, with their mixture of ordered local and random long-range bonds, present the statistical physicist with an interesting percolation model. It turns out that the construction of the original WS model—in which shortcuts are created by reconnecting only one end of an original local bond—renders it analytically hard to treat due to the corre-

lations it introduces between the distribution of local and long-range bonds. For this reason, most analytical work is done using a variant of the model in which long-range bonds are added between randomly chosen pairs of sites. This change does not affect the small-world behavior of the resulting graphs but makes them far easier to treat analytically; we will refer to both the original and the variant as WS models. Figure 1(c) gives an example of a variant WS graph.

Newman and Watts [35] have performed both analytical and numerical analyses of site percolation on such a model with a local bond coordination number k and a density ϕ of shortcuts added per local bond; no local bonds were removed. Their results, suggesting site percolation on WS graphs is similar to that on random graphs, were confirmed by more rigorous work on the same system by Moore and Newman [20,37]. In addition to demonstrating that site percolation on small-world networks is in the same universality class as random graphs (i.e., mean-field), Moore and Newman presented a formal solution to the bond-percolation problem with independent probabilities of local and long-range bonds. They were able to solve this for $k=1$ and $k=2$ to show that the percolation transition in such systems also displays mean-field behavior.

Newman and Moore's results on bond percolation in small-world systems had in fact been anticipated some 17 years earlier by Kaufman and Kardar [36], who solved the bond-percolation problem on what would now be regarded as a $k=1$ WS model with general nearest-neighbor and long-range bond probabilities (p_s,p_l), respectively. In Sec. II of this paper we present a review of Kardar and Kaufman's method and their results describing the percolation transition. In Sec. III we then use the formalism developed in Ref. [36] to consider the critical percolation behavior of a standard WS graph by imposing the relation $p_l=1-p_s$, corresponding to one long-range bond being added to the system for every local bond removed. We then solve the problem for a generalized graph in which we allow the number of long-range bonds added for every short-range bond removed to vary continuously. We also present a brief discussion of percolation on generalized WS graphs defined on k rings and higher-dimensional lattices. An alternative approach to obtaining the results using generating functions is presented in Appendixes A and B.

Recently, some results regarding the appearance of first-order phase transitions in other percolation models in networks were presented in Ref. [38]. Some relevant results on bond percolation in networks were also noted in Ref. [39].

C. Kasteleyn-Fortuin formalism

In Ref. [40] Kasteleyn and Fortuin presented an approach for studying percolation, based on Potts models. In the Potts model, to each site i of the network is assigned a spin s_i with q discrete values of $1,\ldots,q$. Nearest-neighbor spins have an attractive interaction, with a contribution to the energy of $-J\delta_{s_i,s_j}$, where J is a positive constant. In addition, a magnetic field is coupled to all spins, say favoring the sites with $s_i=1$.

The limit $q=2$ of the Potts model is equivalent to the well-known Ising system. For larger values of q the Potts model also exhibits a phase transition but the transition typically becomes first order for large q. An important observation is that, for any value of q, at zero temperature the ground consists of spins pointing in the same direction, whereas when the temperature is increased, the system is separated into clusters of spins pointing at different directions. Kasteleyn and Fortuin observed that at the limit $q\rightarrow 1$ the Potts model reproduces the results of percolation, with the appropriate mapping between the thermodynamic variables and the percolation variables. In the next section this mapping is discussed in detail.

II. PERCOLATION WITH NEAREST-NEIGHBOR AND LONG-RANGE BONDS

A. Model and formalism

Quite generally, the Kasteleyn-Fortuin formalism [40] allows us to relate the bond-percolation problem to the $q\rightarrow 1$ limit of the Potts model. Let us start by considering q-state (Potts) spins s_i on a lattice of N sites. The spins are assumed to be subject to both nearest-neighbor and infinite-range interactions, with a total energy given by the Hamiltonian

$$-\beta\mathcal{H}(K,J,h)=K\sum_{\langle ij\rangle}\delta_{s_i,s_j}+h\sum_i\delta_{s_i,1}+\frac{J}{2N}\sum_{i,j}\delta_{s_i,s_j}. \quad (1)$$

The long-range interaction has to be scaled by $1/N$ to achieve a proper thermodynamic limit, and h is a symmetry-breaking field. The cluster-size generating function is given in terms of the Potts free energy $f(K,h,J)$ by

$$G(p_s,p_l,h)\equiv\sum_{s=1}^{\infty}n_s(p_s,p_l)e^{-sh} \quad (2)$$

$$=-\left.\frac{\partial f}{\partial q}\right|_{q=1}. \quad (3)$$

Here the nearest-neighbor bond-occupation probability is $p_s=1-e^{-K}$, the long-range bond-occupation probability is $2p_l/N=1-e^{-J/N}$ (giving an average of Np_l occupied long-range bonds), n_s is the mean density of s-sized clusters, and $1-e^{-h}$ is the ghost-bond probability. "Ghost bonds" are the percolation equivalent of a magnetic field in the Potts model, and can be considered as connecting each site in the lattice to a single supersite; as a result any nonzero ghost-bond probability automatically results in the formation of an infinite (spanning) cluster since all sites with occupied ghost bonds form part of the same cluster. An example of a cluster involving nearest-neighbor, long-range, and ghost bonds is given in Fig. 2.

The main quantities of interest in percolation are the percolation probability, and the mean finite-cluster size: $P(p_s,p_l)$, is defined as the probability that a site belongs to the infinite cluster while S is the expected size of the cluster of which the site is a member, averaged over all finite-cluster sizes. They are given in terms of $G(p_s,p_l,h)$ by

$$P(p_s,p_l)=1+\frac{\partial}{\partial h}G(p_s,p_l,h=0^+), \quad (4)$$

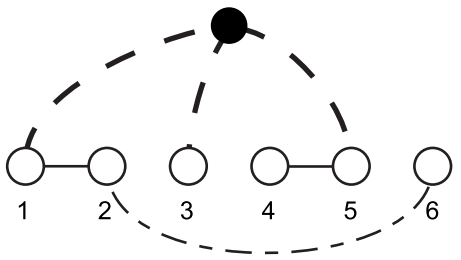

FIG. 2. Example of six sites forming part of a connected cluster with nearest-neighbor bonds (solid lines), long-range bonds (dot-dash), and ghost bonds (dashes). The ghost bonds connect sites (1), (3), and (5) to the ghost supersite, indicated by a black circle. For any finite value of h, a finite proportion of sites in the graph will be connected together via ghost bonds to the supersite, and so all clusters involving ghost bonds must belong to the infinite cluster.

$$S(p_s,p_l) = \frac{\partial^2}{\partial h^2} G(p_s,p_l,h=0^+). \tag{5}$$

To find the free energy of the Potts model, we introduce the partition function

$$Z = \int_{-\infty}^{\infty} \prod_{\alpha=1}^{q} (dx_\alpha e^{-(NJ/2)x_\alpha^2}) \sum_{\{s_i\}} \times \exp\left(K \sum_{\langle ij \rangle} \delta_{s_i,s_j} + \sum_i [(h+Jx_1)\delta_{s_i,1} + \cdots + Jx_q \delta_{s_i,q}] \right). \tag{6}$$

Carrying out the integrals over x and dropping terms of order $\exp[\log N/N]$, we obtain the partition function for the original Hamiltonian introduced in Eq. (1) as

$$Z = \sum_{\{s_i\}} e^{-\mathcal{H}(K,J,h)/kT} = e^{-Nf(K,J,h)}, \tag{7}$$

where $f(K,J,h)$ is the free energy of our Potts model. If instead we first sum over spins in the partition function of the integrand in Eq. (6), we obtain

$$Z = \int_{-\infty}^{\infty} \prod_{\alpha=1}^{q} dx_\alpha \times \exp\left[-(NJ/2) \sum_{\alpha=1}^{q} x_i^2 - N f_0(K,h+Jx_1,\ldots,Jx_q) \right], \tag{8}$$

where $f_0(K,h+Jx_1,\ldots,Jx_q)$ is the free energy of the nearest-neighbor Potts model, $\mathcal{H}(K,J=0,h_1,\ldots,h_q)$, in magnetic fields $h_1=h+Jx_1,\ldots,h_q=Jx_q$.

In the thermodynamic limit $N\to\infty$, a saddle-point method [41] relates the two free energies in Eqs. (7) and (8) by

$$f = \min\left[\frac{J}{2} \sum_{\alpha=1}^{q} x_\alpha^2 + f_0(K,h+Jx_1,\ldots,Jx_q) \right]_{\{x_n\}} = \frac{-J}{2q} + \min\left[Jm + \frac{Jq(q-1)}{2} m^2 + f_0(K,h+qJm) \right]_m, \tag{9}$$

where in the last line we have used the observation that the x_α are the magnetizations of the Potts model [36,41] and introduced a parametrization

$$x_1 = 1/q + (q-1)m, \quad x_2 = \cdots = x_q = 1/q - m.$$

Setting $q=1$ and using Eq. (3), we obtain the cluster-size generating function for percolation with nearest-neighbor and long-range bonds,

$$G(p_s,p_l,h) = -\min[p_l(m-1)^2 - G_0(p_s,h+2p_l m)]_m, \tag{10}$$

where $G_0(p,h)$ is the cluster-size generating function for percolation with only nearest-neighbor bonds. We note that $\bar{m}$, the value of m that minimizes the expression in Eq. (10), is the percolation probability P.

It is simple to calculate the function $G_0(p,h)$ in one dimension using Eq. (2); to form an s-size cluster requires a sequence of $(s-1)$ occupied bonds with an empty bond at each end to terminate the sequence. Thus $n_s=(1-p_s)^2 p_s^{s-1}$, and performing the sum we find

$$G_0(p_s,h) = \frac{(1-p_s)^2}{e^h - p_s}. \tag{11}$$

Substituting this result into Eq. (10) we obtain the generating function for bond percolation on a graph with nearest-neighbor and long-range bonds,

$$G(p_s,p_l,h) = -\min\left[p_l(m-1)^2 - \frac{(1-p_s)^2}{e^{h+2p_l m} - p_s} \right]_m. \tag{12}$$

This is the result that we shall be using for the rest of this paper; we note that for percolation in the context of small-world networks only the $h\to 0^+$ limit is relevant.

B. Mean-field percolation

Given that in the vicinity of the percolation transition we expect $P=\bar{m}$ to be small, we can perform an expansion of Eq. (12) in powers of m to give (taking $h=0$)

$$G(p_s,p_l,0) = 1 - p_s - p_l \min\left\{ p_l m^2 \left[1 - 2p_l \frac{1+p_s}{1-p_s} \right] + \frac{4p_l^3 m^3}{3} \frac{1+4p_s+p_s^2}{(1-p_s)^2} + \mathcal{O}(m^4) \right\}_m. \tag{13}$$

The phase transition thus occurs when the coefficient of m^2 changes sign, giving a transition boundary

$$2p_l = \frac{1-p_s}{1+p_s}. \tag{14}$$

Note that, since m cannot be negative, the presence of a cubic term does not imply a first-order transition. Defining

$$t = 2p_l\left(\frac{1+p_s}{1-p_s}\right) - 1, \tag{15}$$

we find the critical behavior at the transition to be

$$G^{\text{sing}} \sim \begin{cases} 0, & t<0, \\ t^3, & t>0, \end{cases} \tag{16}$$

$$P = \bar{m} \sim \begin{cases} 0, & t<0, \\ t, & t>0, \end{cases} \quad \text{and} \tag{17}$$

$$S \sim t^{-1}. \tag{18}$$

Using the standard definitions [42], $G^{\text{sing}} \sim t^{2-\alpha}$, $P \sim t^{\beta}$, and $S \sim t^{-\gamma}$, this gives critical exponents

$$\alpha = -1, \quad \beta = 1, \quad \text{and} \quad \gamma = 1, \tag{19}$$

typical of mean-field behavior [43,44], in agreement with the results of Moore and Newman [37,45].

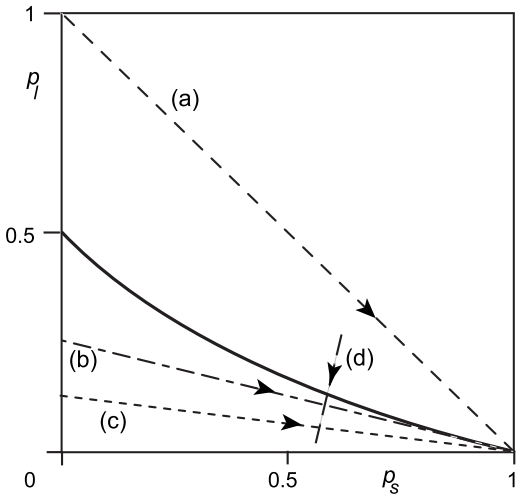

FIG. 3. Small-world trajectories: the lines (a)–(c) show examples of small-world trajectories superimposed on the phase diagram of the more general percolation system. The arrows show the direction of *decreasing* p. Trajectory (d) shows a nonsmall-world trajectory for which mean-field behavior holds at the transition. Trajectory (a), with $n=1$, corresponds to the standard Watts-Strogatz graph and is clearly always percolating. Trajectories (b) and (c), with $n=1/4$ and $n=1/8$, respectively, are always in the nonpercolating regime.

III. GENERALIZED WATTS-STROGATZ GRAPHS

A. Percolation

The results of Sec. II, describing percolation with general nearest-neighbor and long-range bond-occupation probabilities, give a solution to the bond-percolation problem as defined on a small-world graph [20,37] but are not quite appropriate to describing the percolative behavior of the graph itself. Recall that, in the Watts-Strogatz model, the proportions of long-range and nearest-neighbor bonds are not independent but rather a fraction p of nearest-neighbor bonds is replaced with long-range bonds. Thus p_l and p_s are firmly connected by the relationship $p=p_l=(1-p_s)$. For any value of p, the WS graph occupies a point in the (p_s,p_l) configuration space of the more general model which satisfies this relation, and varying p describes a trajectory through this configuration space [see Fig. 3(a)]. The appropriate equation for describing the percolative behavior of the $k=1$ (nearest-neighbor) Watts-Strogatz graph is, therefore, given by substituting for p_s and p_l in Eq. (12), giving us the cluster-size generating function for the WS model as

$$G(n,p,h) = -\min\left[p(m-1)^2 - \frac{p^2}{e^{h+2pm}-1+p}\right]_m. \tag{20}$$

According to Eq. (15), the controlling parameter t for this system is given by $t=3-p \Rightarrow 2 \le t \le 3$, and, therefore, we expect the system to lie deeply in the percolating phase for all values of p. Nonetheless, it is not difficult to solve Eq. (20) numerically, and the resulting graphs of G, P, and S as a function of p are illustrated in Fig. 4. The divergence of S as $p \to 0$ indicates that $p=0$ represents some kind of critical point. Additional evidence for this comes from the fact that, while P comes in linearly to the limiting value $P=\sqrt{3}/2 \approx 0.866$ as $p \to 0$, at the exact point $p=0$ the bond configuration of the system is that of a completely connected linear chain and, therefore, $P=1$ is the only physically acceptable value. Therefore, we are faced with a divergence in S and a discontinuity in P at $p=0$. Taken together with the fact that p is the only free parameter in the system once we have set $h=0$, it is reasonable to take p rather than t to be the appropriate control parameter for percolation in the WS network.

With this in mind, we can compare the more general results of Eqs. (16)–(18) to the $p \to 0$ behavior of the WS network, as indicated by Fig. 4,

$$G \sim p,$$

$$P \sim \text{const},$$

$$S \sim p^{-1}. \tag{21}$$

Evidently, only S performs according to the mean-field predictions; G is linear in p rather than the expected cubic behavior while P is constant rather than linear. Therefore, in this limit the WS network exhibits critical exponents $\alpha=1$, $\beta=0$, and $\gamma=1$ in contrast to the mean-field values in Eqs. (19). We note for future reference that the critical exponents found for the WS network satisfy the scaling exponent identity $\alpha+2\gamma+\beta=2$.

Thus, the above results demonstrate that the WS graph exhibits an unusual transition as $p \to 0$. Rather than the generic mean-field behavior typical of percolation with general short- and long-range bond probabilities, the WS network displays a transition between two percolating phases, with P jumping discontinuously from a finite value to unity while S

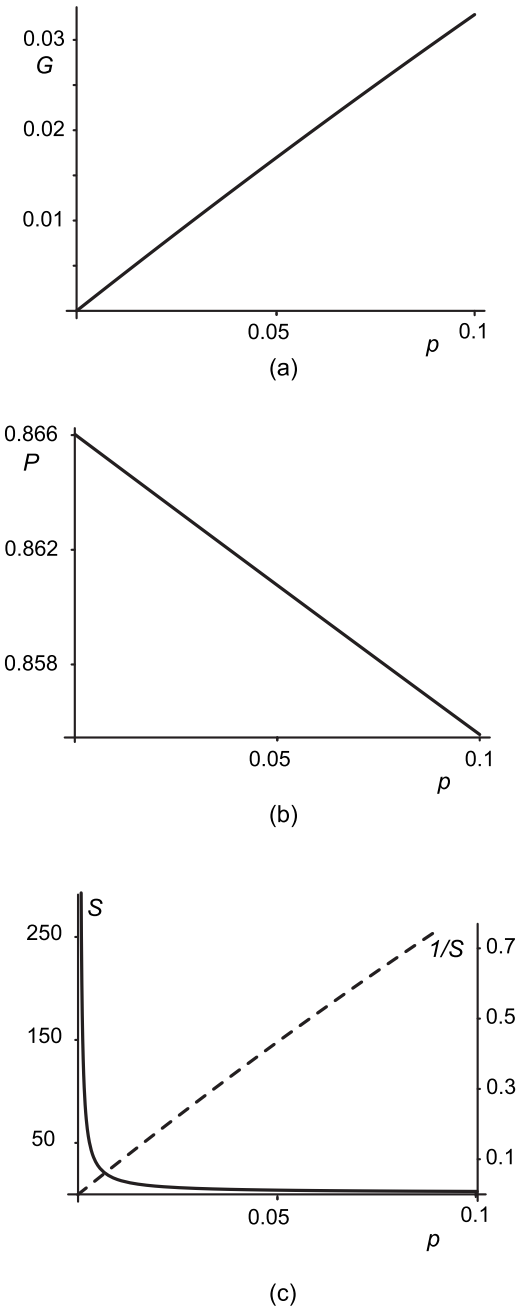

FIG. 4. Numerical results for the standard ($n=1$) Watts-Strogatz network: (a) cluster size generating function $G(p)$, (b) percolation probability $P(p)$, and (c) the mean finite-cluster size $S(p)$.

diverges continuously as $1/p$. In the following section, by considering a generalization of this model we provide an analytical explanation for this behavior.

B. Scaling

The original choice of Watts and Strogatz, fixing the number of added long-range bonds to equal the number of short-range bonds that were removed, was motivated by the desire to compare the properties of graphs having the same total number of bonds for different values of p. However, when applying their model to physical systems, there is no reason *a priori* to assume this to be the case. In some cases long-range bonds are more "costly" than short-range bonds and we would expect the relative number of long-range bonds in the system to be fewer. Alternatively, in the context of neural connections, suitable training of a growing cortex can result in a relative increase in the number of long-range bonds.

With these considerations in mind, we now define a generalized WS graph by the simple expedient of allowing the number of long-range bonds added for every short-range bond removed to vary continuously; Fig. 1(d) gives an example of such a generalized graph. Thus for such graphs, the relationship between p_s and $p=p_l$ is given by

$$p = p_l = n(1 - p_s). \tag{22}$$

An illustration of some of the trajectories for different values of n is given in Fig. 3. Substituting Eq. (22) into Eq. (12) gives us the cluster-size generating function for nearest-neighbor generalized Watts-Strogatz graphs,

$$G(n,p,h) = -\min[f(m,n,p,h)]_m, \tag{23}$$

where for convenience we have defined

$$f(m,n,p,h) = p(m-1)^2 - \frac{(p/n)^2}{e^{h+2pm} - 1 + p/n}. \tag{24}$$

We now restrict our attention to trajectories along which P is small in the $p \to 0$ limit, which we expect to be those in the immediate vicinity of, and beneath, the transition line in Fig. 3. While the restriction on m being small means that any results derived using it are not strictly applicable to the $n=1$ case treated numerically in Sec. III A, we expect that universal quantities such as critical exponents should agree in both cases. With this in mind, we make a small-m expansion of Eq. (24) to give the equivalent of Eq. (13).

We start with the case $h=0$. The free energy then becomes

$$f(m,n,p,h=0) = p\left(1 - \frac{1}{n}\right) + pm^2(1 + 2p - 4n) + \frac{4}{3}pm^3(6n^2 - 6pn + p^2). \tag{25}$$

Considering the coefficient of m^2, we immediately see that the percolation transition occurs when

$$n = \frac{1+2p}{4}. \tag{26}$$

Therefore, in the $p \to 0$ limit, the transition line in Fig. 3 comes down linearly with a slope of $-1/4$. As in Eq. (13), the presence of a cubic term does not imply a first-order transition since $\bar{m}=P$ is confined to the range (0,1). Defining $\delta_n = n - 1/4$, and setting $\partial f/\partial m = 0$ to obtain $\bar{m}$, we find

$$P = \bar{m} = \begin{cases} 0 & n < \frac{1}{4}(1+2p) \\ \dfrac{4\delta_n - 2p}{12n^2 - 12np + 2p^2} & n > \frac{1}{4}(1+2p) \end{cases}. \tag{27}$$

This result is only valid for $\bar{m} \ll 1$, and so it follows that our expression for f in Eq. (25) is only valid for $n \lesssim 1/4$. We can

write the singular parts of G and P in the $p \to 0$ limit as

$$G^{\text{sing}}(p \to 0;n) \sim \begin{cases} 0, & \delta_n \leq p/2, \\ p\delta_n^3, & \delta_n > p/2, \end{cases} \tag{28a}$$

$$P(p \to 0;n) = \bar{m} \sim \begin{cases} 0, & \delta_n \leq p/2, \\ 4\delta_n - 2p, & \delta_n > p/2. \end{cases} \tag{28b}$$

Once again, these results are quite distinct from the mean-field predictions of Eqs. (16) and (17). Moreover, the results for $\delta_n > p/2$, giving $\alpha=1$ and $\beta=0$ with P tending linearly to a finite constant as $p \to 0$, are in accordance with the numerically obtained behavior of Eqs. (21), arguing for the universality of Eqs. (28a) and (28b) at all $n > 1/4$

Note that the result from Eq. (28b), in which increasing p reduces the percolation probability, should not be surprising since the total number of bonds in the system is proportional to $(p_l+p_s)=1+p(1-1/n)$. Therefore, for $n<1$, increasing p reduces the total number of bonds in the system. This can also be understood by considering the convex nature of the transition line in Fig. 3; all trajectories with $\frac{1}{4}<n<\frac{1}{2}$ will intersect the line twice: once at $p=0$ and again at $p \approx 2\delta_n$. Moreover, the second transition does behave in the mean-field manner, meaning that $P \to 0$ linearly as we approach it. Since when $\delta_n \ll 1$ the distance between the two transitions becomes vanishingly small, the percolation probability P must decrease from $P=4\delta_n$ to $P=0$ linearly as we increase p through the increment from 0 to $\delta_n/2$.

We now turn to calculating the mean finite-cluster size, S, which is the equivalent of the susceptibility for a percolation system. Equations (4) and (5) imply that we can write

$$S = \left. \frac{\partial \bar{m}}{\partial h} \right|_{h=0^+}. \tag{29}$$

We, therefore, need to find the h dependence of $\bar{m}$. This is simple to do if we notice that by defining

$$\hat{m} = m + \frac{h}{2p},$$

we may express $f(m,h)$ as

$$f(m,h) = f(\hat{m},0) - \frac{h^2}{4p} + h\hat{m} + h. \tag{30}$$

Expanding G for small p, m, δ_n, and h, we find

$$G = p \min\left[\frac{3}{4} + \frac{h}{2p} + 2m^2(p-2\delta_n) + \frac{mh}{p}(2p-4\delta_n-1) + \frac{h^2}{4p^2}(2p-4\delta_n-1) + \frac{1}{2}\left(m - \frac{h}{2p}\right)^3 \right]_m. \tag{31}$$

Minimizing the free energy with respect to m and expanding to lowest orders in p, δ_n, and h, one obtains the magnetization as

$$\bar{m} = \begin{cases} \dfrac{h}{p(4p-8\delta_n)}, & \delta_n \leq p/2, \\ \dfrac{16\delta_n - 8p}{3} - \dfrac{h}{p(4p-8\delta_n)}, & \delta_n > p/2. \end{cases} \tag{32}$$

Substituting this value into Eq. (31), we get the free-energy expression near the singular point as

$$G = p\left(\frac{3}{4} + \frac{h}{2p} - \frac{3h^2}{8p^2(2\delta_n - p)} \right), \tag{33}$$

for $\delta_n \leq p/2$, and

$$G = p\left(\frac{3}{4} + \frac{8^3}{2(3^3)}(2\delta_n - p)^3 + \frac{h}{2p} - \frac{3h^2}{8p^2(2\delta_n - p)} \right), \tag{34}$$

for $\delta_n > p/2$. This implies that the singular part of the free energy can be written as

$$G^{\text{sing}} = p^4 x^3 \phi_x(\tilde{h}), \tag{35}$$

where

$$x = \frac{\delta_n}{p} - \frac{1}{2}, \tag{36}$$

$$\tilde{h} = \frac{h}{p^3 x^2}, \tag{37}$$

and ϕ is a universal scaling function, obeying

$$\phi_x(\tilde{h}) \sim \begin{cases} \tilde{h}^2 & x \leq 0, \\ \dfrac{3}{2} - \tilde{h} & x > 0. \end{cases} \tag{38}$$

Therefore, in the $p \to 0$ limit, we find the critical behavior of S as $p \to 0$ to be

$$S(p \to 0;n) \sim \begin{cases} -n/(2\delta_n p) & \delta_n < p/2, \\ (1/2-n)/(2\delta_n p) & \delta_n \gtrsim p/2, \\ 1/(4p^2) & \delta_n = p/2. \end{cases} \tag{39}$$

The critical exponent for the divergence of S is, therefore, $\gamma=1$ for $\delta_n \neq p/2$, and $\gamma=2$ for $\delta_n=p/2$. These results for S show a number of interesting points. The first is that, for $\delta_n \neq p/2$, S diverges in agreement both with the mean-field prediction and the numerical result for $n=1$. We also note that the amplitude for the divergence at $\delta_n=p/2^+$ is equal to that for $\delta_n=p/2^-$. However, for $\delta_n=p/2$ precisely, the percolation transition is accompanied by a different divergence in S. Thus, while G and P display the same singular behavior for $\delta_n=p/2$ and $\delta_n<p/2$, the two cases are differentiated by the order of divergence in S.

C. Other lattices

Given the rich behavior of percolation on the simple WS model, it is natural to enquire if similar behavior exists when the underlying lattice structure is of a higher dimension. Re-

turning to the considerations of Sec. II, we note that to treat the higher-dimensional case all we need do is to substitute the appropriate G_0 into Eq. (10). Unfortunately, the exact form of G_0 is not known for dimensions higher than one (not counting the infinite-dimensional Bethe lattice), and so an analytic solution of the higher-dimensional case is not possible by this method. Nevertheless, enough is known about the properties of $G_0(p_s,h)$ in higher dimensions to make some general statements about percolation in such graphs. In particular, close to the percolation transition we can write a form equivalent to the expansion in Eq. (13), as

$$G(p_s,p_l,0) = -p_l + G_0(p_s,0) - \min_m \left\{ p_l m^2[1 - 2p_l S_0(p_s)] + \frac{4}{3}p_l^3 U_0(p_s)m^3 + O(m^4) \right\},$$

where $S_0 = \partial^2 G_0/\partial h^2|_{h=0^+}$ is the mean finite-cluster size of the nearest-neighbor model on the underlying lattice, and $U_0 = -\partial^3 G_0/\partial h^3|_{h=0} > 0$. There will thus be a percolation transition at the point $2p_l = S_0^{-1}$, again governed by mean-field exponents.

This result provides enough information to draw some conclusions about the behavior of generalized WS graphs in higher dimensions. In particular, in the one-dimensional case it was the intersection of small-world trajectories with the critical point at $p=0$ that gave rise to all the interesting behavior as $p \to 0$. In higher dimensions, however, small-world trajectories as defined in Eq. (22) do not encounter any critical points as $p \to 0$. Thus, we would not expect any critical behavior other than a mean-field transition should they pass through the transition line [in the (p_l,p_s) space] at some point other than the origin.

IV. CONCLUSION AND DISCUSSION

We have examined the percolation properties of a class of WS graphs generalized by allowing the proportion of long-range and short-range bonds to vary with a parameter n according to $p_l = n(1-p_s) \equiv p$. Such graphs then lie along small-world trajectories parametrized by n and p in the space of graphs with general (p_s,p_l). Previous solutions of bond percolation on graphs with general (p_s,p_l) have been shown to give results in the same class as random graphs [20,36,37], with the transition between the percolating and nonpercolating phases controlled by mean-field exponents $\alpha=-1$, $\beta=1$, and $\gamma=1$.

An interesting aspect of the original Watts-Strogatz model, and its generalization presented here is the interplay between the deleted short-range links and the added shortcuts. In this paper we have discussed several aspects of this interplay, including the discontinuous jump between the two *percolating* phases at $p=1$ and the critical behavior near the percolation phase-transition point.

We have presented an analytical solution of generalized WS graphs, valid for $n \lesssim 1/4$, and a numerical solution for the standard $(n=1)$ WS graph, which together show that the critical behavior of such networks in the $p \to 0$ limit falls into one of three regimes of behavior depending upon the value of n. Moreover, in none of these regimes is the transition described by standard mean-field. Trajectories for which $n > 1/4$ display a transition between two percolating phases in which the percolation probability, P, jumps discontinuously from a finite value to unity at the transition point while the mean finite-cluster size, S, diverges. The critical exponents associated with the transition are $\alpha=1$, $\beta=0$, and $\gamma=1$. Trajectories with $n<1/4$ and $n=1/4$ both display a percolation transition with a P jumping discontinuously from zero to one, and critical exponents $\alpha=2$ [46] and $\beta=0$; however they are differentiated by the behavior of S, which diverges with exponent $\gamma=1$ for $n<1/4$ and $\gamma=2$ for $n=1/4$.

We have further proposed that all three regimes of behavior can be unified within a single scaling form for the cluster-size generating function, G, which is valid in the vicinity of the critical point $p=0$. According to this proposal, the failure of the critical exponents for $n \leq 1/4$ to satisfy the identity $\alpha+2\beta+\gamma=2$ can be related to asymptotic zeros of the scaling function. We have also considered the percolative behavior of generalized WS graphs on higher-dimensional lattices. While no exact solution exists, general considerations of the form of the phase diagram for systems with general $(p_s,p_l s)$ indicate that there should not be any critical behavior along small-world trajectories.

To conclude, we note that, as far as we are aware, studies of the dependence of the graph diameter, l, on the long-range bond probability p in WS graphs have so far focused exclusively on the $n=1$ case. However, our analysis of bond percolation in generalized WS graphs has shown that varying n can have important consequences in case of a one-dimensional underlying lattice. In particular, according to the form of our scaling function, in the $p \to 0$ limit it is the quantity $(n-1/4)/p$ that is the physically important parameter in percolation. An interesting question, therefore, arises as to whether the graph diameter $l(p)$ has a corresponding dependence on n, and in particular whether the value $n=1/4$ has a physical significance beyond the percolation behavior presented here.

It should be noted that the original WS model has been extended mainly to k rings, rings where each node is connected to its k nearest neighbors on each side (for a total of $2k$ nearest neighbors bonds per site). While this model is also one dimensional, and does not percolate without long-range bonds (unless $p_s=1$), the singular behavior as $p \to 0$ could well be different from the case $k=1$. For a k ring, a lower bound on the asymptotic probability that a node does not belong to a long "supernode" extending to its left behaves as $(1-p_s)^k$. Using Eq. (A6) with p_s' replacing p_s, and with the approximation $1-p_s' \sim (1-p_s)^k$, one obtains that for $k>1$, $y \to 0$ for $p_s \to 1$. Therefore, the behavior near the fully connected ring state is analytic—in contrast to the singly connected ring, no jump discontinuity exists.

ACKNOWLEDGMENT

M.K. is supported by NSF Grant No. DMR-04-26677.

APPENDIX A: GENERATING FUNCTION APPROACH

In this Appendix we develop a different approach to studying the percolation transition in small-world networks.

We use the generating function formalism, stressing the topological rather than thermodynamic structure of the network. The percolation process can be perceived as consisting of two stages. In the first stage short-range links are removed from the network with probability $1-p_s$. The remaining network consists of isolated islands of varying sizes. We will term a group of nodes connected by a chain of short-range links a supernode. This construction can be viewed as a renormalization of the network, where each supernode is a node in the new network, having weight proportional to its original size. In the second stage long-range links are added to the network, and we study the connectivity between supernodes through these long-range links. The probability, $P(d)$, of a node to belong to a supernode of size d is the number of possible consecutive sets of size d including this node (which is just d) times the probability of the $d-1$ links between these d nodes to be intact, and the two links leading to nodes neighboring this supernode to be removed. Therefore,

$$P(d) = dp_s^{d-1}(1-p_s)^2, \tag{A1}$$

and the generating function for the supernode size is

$$S(x) = \sum_{d=1}^{\infty} dp_s^{d-1}(1-p_s)^2 x^d = \frac{x(1-p_s)^2}{1-xp_s}. \tag{A2}$$

Consider now the distribution of the number of long-range links emanating from a supernode of size d; since there are $p_l N$ edges having $2p_l N$ ends (links) randomly distributed on the ring, we expect a Poisson distribution of the links with mean $2p_l$ per node, or $2dp_l$ per supernode. Therefore, the probability of having k links from a supernode is

$$P(k|d) = \frac{(2dp_l)^k e^{-2dp_l}}{k!}, \tag{A3}$$

and the joint generating function for supernode size and degree is

$$D(x,y) = \sum_{d,k} P(d)P(k|d)x^d y^k = (1-p_s)^2 \frac{xe^{2p_l(y-1)}}{(1-p_s xe^{2p_l(y-1)})^2}. \tag{A4}$$

To calculate the distribution of component sizes obtained by following a link, one should notice that the probability of reaching each node by following a long-range link is the same. Therefore, the probability of reaching a supernode is proportional to its size and similar to the probability that a node belongs to a supernode of size d. Hence, the distribution of cluster sizes reached by following a link (which is similar to the distribution of cluster sizes in general due to the Poisson distribution) is given by the self-consistent equation

$$y = D(x,y). \tag{A5}$$

From this self-consistency condition all cluster and percolation properties can be obtained. In particular, when finding the solution of the equation

$$y_p = D(1,y_p), \tag{A6}$$

if $y_p=1$ there exists no giant component while for $y_p<1$ a giant component exists. The size of the giant component is determined to be $S=1-y_p$. As discussed before, the behavior as $p_s \to 1$, with $p_l=1-p_s$ is special: as this limit is approached, $S \to \frac{\sqrt{3}}{2} \approx 0.866$, with a discontinuous jump to $S=1$ for $p_s=1$ and $p_l=0$.

Expanding Eq. (A5) in powers of ϵ for $y=1-\epsilon$ and $x=1$ gives the phase-transition behavior for the model. One obtains

$$1-\epsilon = 1 + \frac{2p_l(p_s+1)}{p_s-1}\epsilon + \frac{4p_l^2(p_s^2+4p_s+1)}{2(p_s-1)^2}\epsilon^2 + \ldots, \tag{A7}$$

leading to the critical percolation threshold at

$$\frac{2p_l(p_s+1)}{1-p_s} = 1. \tag{A8}$$

Near the threshold it can be seen that the quadratic term in ϵ will always exist unless $p_s \to 1$ or $p_l \to 0$. For a generalized n the behavior depends on the expansion of the linear terms in ϵ as a function of the deviation from the critical point. Furthermore, for the original WS model with $p=p_l=1-p_s$ it is easily seen that the whole $0 \le p \le 1$ range is within the percolating regime.

APPENDIX B: CRITICAL EXPONENTS FOR THE k RING

A full analytic solution of the k-ring problem is complicated, as there any many different possible configurations for a connected component. It is, therefore, difficult to account for all possible cluster structures. An extreme simplification that allows for exact solution is a ring in which every pair of nearest neighbors is connected by k links rather than one.

Let us begin with a configuration in which each node is connected to each of its two nearest neighbors with k links. Then, a fraction $1-p_s'$ of the short-range links is removed and with probability $p_l'=n(1-p_s')$ a long-range links is added. As the number of links in the initial ring is now Nk, the total number of long-range links added is Nkp_l'. The probability of disconnecting a pair of near neighbors is $(1-p_s')^k$. Thus, this model is equivalent to the singly connected ring with

$$p_l = kp_l', \tag{B1}$$

and

$$p_s = 1-(1-p_s')^k. \tag{B2}$$

For $k=1$ this model is simply the singly connected ring studied before. For $k>1$, one may use previous results, such as Eq. (A8) in conjunction with Eqs. (B1) and (B2), to find the percolation threshold and other properties of the network. In the limit of $p_s \to 1$ this behaves similarly to the one-ring case, with $n \to \infty$, as the ratio of added shortcuts to removed short-range links becomes infinite. This leads to the formation of dense graphs of supernodes, and thus the singularity at $p_s \to 1$ vanishes.

[1] S. Milgram, Psychol. Today **2**, 60 (1967).
[2] For example, a current attempt is made to conduct an experiment similar to Milgram's at the facebook web site. See http://www.steve-jackson.net/six_degrees/index.html for more information.
[3] B. Bollobás, *Random Graphs* (Academic Press, New York, 1985).
[4] M. Granovetter, Am. J. Sociol. **78**, 1360 (1973).
[5] D. J. Watts and S. H. Strogatz, Nature (London) **393**, 440 (1998).
[6] M. E. J. Newman and D. J. Watts, Phys. Lett. A **263**, 341 (1999).
[7] M. E. J. Newman, C. Moore, and D. J. Watts, Phys. Rev. Lett. **84**, 3201 (2000).
[8] C. F. Moukarzel, Phys. Rev. E **60**, R6263 (1999).
[9] N. Mathias and V. Gopal, Phys. Rev. E **63**, 021117 (2001).
[10] A.-L. Barabási and R. Albert, Science **286**, 509 (1999).
[11] B. Bollobas and O. Riordan, in *Handbook of Graphs and Networks*, edited by S. Bornholdt and H. G. Schuster (Wiley-VCH, Weinheim, Germany, 2002).
[12] R. Cohen and S. Havlin, Phys. Rev. Lett. **90**, 058701 (2003).
[13] S. N. Dorogovtsev, J. F. F. Mendes, and A. N. Samukhin, Nucl. Phys. B **653**, 307 (2003).
[14] L. A. N. Amaral, A. Scala, M. Barthélémy, and H. E. Stanley, Proc. Natl. Acad. Sci. U.S.A. **97**, 11149 (2000).
[15] A. Barrat and M. Weigt, Eur. Phys. J. B **13**, 547 (2000).
[16] K. Malarz, Int. J. Mod. Phys. C **14**, 561 (2003).
[17] L. F. Lago-Fernández, R. Huerta, F. Corbacho, and J. A. Sigüenza, Phys. Rev. Lett. **84**, 2758 (2000).
[18] S. A. Pandit and R. E. Amritkar, Phys. Rev. E **63**, 041104 (2001).
[19] S. Jespersen, I. M. Sokolov, and A. Blumen, Phys. Rev. E **62**, 4405 (2000).
[20] C. Moore and M. E. J. Newman, Phys. Rev. E **61**, 5678 (2000).
[21] M. Kuperman and G. Abramson, Phys. Rev. Lett. **86**, 2909 (2001).
[22] M. J. Keeling and K. T. D. Eames, J. R. Soc., Interface **2**, 295 (2005).
[23] E. M. Rauch and Y. Bar-Yam, Phys. Rev. E **73**, 020903(R) (2006).
[24] Y. Bar-Yam and I. R. Epstein, Proc. Natl. Acad. Sci. U.S.A. **101**, 4341 (2004).
[25] M. A. M. de Aguiar, I. R. Epstein, and Y. Bar-Yam, Phys. Rev. E **72**, 067102 (2005).
[26] D. Braha and Y. Bar-Yam, Manage. Sci. **53**, 1127 (2007).
[27] J. Z. Chen and J. Y. Zhu, Chin. Phys. Lett. **24**, 839 (2007).
[28] J. Kleinberg, Nature (London) **406**, 845 (2000).
[29] R. Albert and A.-L. Barabási, Rev. Mod. Phys. **74**, 47 (2002).
[30] R. Pastor-Satorras and A. Vespignani, *Evolution and Structure of the Internet: A Statistical Physics Approach* (Cambridge University Press, Cambridge, 2004).
[31] S. N. Dorogovtsev and J. F. F. Mendes, Adv. Phys. **51**, 1079 (2002).
[32] M. E. J. Newman, SIAM Rev. **45**, 167 (2003).
[33] S. N. Dorogovtsev and J. F. F. Mendes, *Evolution of Networks: From Biological Nets to the Internet and WWW* (Oxford University Press, Oxford, 2003).
[34] S. Galam and K. Malarz, Phys. Rev. E **72**, 027103 (2005).
[35] M. E. J. Newman and D. J. Watts, Phys. Rev. E **60**, 7332 (1999).
[36] M. Kaufman and M. Kardar, Phys. Rev. B **29**, 5053 (1984).
[37] C. Moore and M. E. J. Newman, Phys. Rev. E **62**, 7059 (2000).
[38] D. Achlioptas, R. M. D'Souza, and J. Spencer, Science **323**, 1453 (2009).
[39] J. Gleeson, e-print arXiv:0904.4292.
[40] P. W. Kasteleyn and C. M. Fortuin, J. Phys. Soc. Jpn. **26** (supplement), 11 (1969).
[41] M. Kardar, Phys. Rev. B **28**, 244 (1983).
[42] D. Stauffer and A. Aharony, *Introduction to Percolation Theory*, 2nd ed. (Taylor & Francis, London, 1992).
[43] F. Y. Wu, J. Appl. Phys. **53**, 7977 (1982).
[44] M. E. Fisher and J. W. Essam, J. Math. Phys. **2**, 609 (1961).
[45] Readers comparing these exponents to the ones in the paper by Moore and Newman [37] should note their nonstandard exponents σ and τ. In standard percolation language, $\tau_{\mathrm{MN}}=(\tau_{\mathrm{perc}}-1)$ and $\sigma_{\mathrm{MN}}=1/\gamma_{\mathrm{perc}}$. For a full treatment of the definitions of critical exponents in percolation, see Ref. [42].
[46] Readers familiar with one-dimensional percolation will be surprised to see us claim that $\alpha=2$ for the $n=0$ case rather than the accepted result $\alpha=1$. The discrepancy arises because the term in G that is linear in p is independent of δ_n and $\bar{m}$, and so has been excluded from our definition of G^{sing}. Another point to bear in mind is that our formulation of the model is ill suited to dealing with $n=0$ due to the numerous $1/n$ terms in Eq. (23) that arise from our definition of n. If instead we simply set $p_l=0$ in Eq. (3), no such problems arise.